ELSEVIER

Precambrian Research 84 (1997) 63–81

Precambrian Research

Tidal sandwaves and related storm deposits in the transgressive Protoproterozoic Chaibasa Formation, India

Pradip K. Bose *, Rajat Mazumder, Subir Sarkar

Department of Geological Sciences, Jadavpur University, Calcutta 700 032, India

Received 6 August 1996; accepted 19 February 1997

Abstract

Despite deformation and metamorphism the 2.3 Ga fine-grained siliciclastic Chaibasa Formation of eastern India locally retains an excellent record of sandwave migration under the influence of tides and storms within a precursor sandstone facies in a largely subtidal setting and provides a rare opportunity to detect tidal periodicities.

In the finer facies locally preserved, minor features provide glimpses of the depositional mechanisms and settings. The silt-dominated precursor heterolithic (silt-mud) facies contain numerous slides and slumps and was formed on a relatively steep slope between the fairweather and storm wave bases. The shale facies formed in a deeper setting beneath the wave base. Earthquakes occasionally have interrupted normal sedimentation and massflow products are present in all the facies, but with increasing frequency within the finer facies.

The sandstone facies units, which were emplaced during repeated lowstands, were first subjected to progradation and subsequently drowned, in an overall transgression trend. © 1997 Elsevier Science B.V.

Keywords: Protoproterozoic; Chaibasa; Tidal periodicities; Storm; Turbidites; Punctuated transgression

1. Introduction

Deformation and metamorphism obscure sedimentation patterns and depositional sequences in older Precambrian successions, as in the 2.3 Ga Chaibasa Formation in eastern India. A fortuitous retention of primary structures in patches within the Formation, however, provides a rare opportunity to have a glimpse of depositional mechanisms during an early phase of the Earth's history. Pertaining to this, among other things, are incontrovertible tidal periodicities which the workers on the early Earth–Moon system (e.g. Williams, 1989; Archer, 1996; Chan et al., 1994; Sonett et al., 1996) may find useful and informative. A poor sedimentological account of the Formation, which has comprised entirely of micaschists sparsely interbedded with quartzite of average thickness 20 m, have led to an absurd range of paleogeographic interpretations from fluvial to deep sea (Table 1). Without any rigorous sedimentological analyses, the interpretations are based on cursory observations and intuition (see the evaluation in Table 1). A reappraisal of the paleogeography has thus been carried out and a plausible mode of sequence-building has been inferred from an integrated analysis of the available observations.

The precursor lithology of the Formation is

* Corresponding author at: 25/29A Prince Golam, Md. Shah Road, Calcutta 700 045, India.

PII S0301-9268(97)00016-8

Table 1
Paleogeographic models for the Chaibasa Formation

Author	Paleogeography	Brief evaluation
Mathur (1960)	Deep marine	Some workers emphasized graded Sst beds, others missed them. Some ignored the implication of large scale cross-beddings. Sh–siltstone interbedding/laminae was interpreted by some as turbidite-pelagite alternations and by others as products of tidal energy fluctuations. Some put emphasis on rare spindle-shaped silt-filled cracks (whose proclaimed desiccation origin is not beyond doubt amid the profusion of water escape structures). The overall paleocurrent in Sst was, according to some, unimodal and to others bimodal. Some workers, despite claiming the Sst as flysch, did not account for the high textural and mineralogical maturity. Critical and integrated sedimentological analysis was lacking.
Naha (1961)	Deep marine	
Sarkar and Saha (1962)	Shallow to deep marine	
Gaal (1964)	Largely shallow marine	
Sarkar and Saha (1986)	Moderately deep marine	
Bhattacharya (1991)	Peritidal	
Sarkar et al. (1992)	Shallow marine environment	
Virnave et al. (1994)	Fluvial	
Bose (1994)	Relatively deep marine	

confined within the range between fine sandstone, siltstone and shale. Soft sediment deformation structures frequently occur particularly within the siltstones,along selective stratigraphic levels traceable over the entire outcrop lengths ranging up to ca 1 km (Naha, 1956; Ghosh and Lahiri, 1983). Three successive sandstone units encased by finer sediments could be studied in detail only on the unfolding of the strata in an 11-km stretch between 1.2 km west of Maubhandar and 2 km east of Ghatshila (Fig. 1b). The finer lithologies are intensely overprinted by meta- and post-depositional deformations yet some tell-tale primary characteristics of these were recorded from selected patches in the area between Galudih and Dhalbhumgarh (Fig. 1a).

2. Geological setting

The 6–8 km thick Chaibasa Formation in eastern India, which is entirely fine-grained siliciclastic [ca 2300–2400 Ma, Saha et al. (1988); Sarkar and Saha (1962)], has been deformed and metamorphosed to greenschist and locally amphibolite facies [Naha (1965); Saha (1994); Fig. 1]. It directly overlaps the granitic basement on its southeastward extension overrunning the coaxially-folded Dhanjori Formation [Fig. 1a; Sarkar (1984); Basu (1985); Gupta et al. (1985)]. The fold plunges north-westward (Naha, 1965). Naha (1961) measured paleocurrent directions from the precursor Chaibasa sandstones after removing the plunge and unfolding the strata, as has been done throughout this paper to achieve compatible results. Besides the studies on paleocurrent and soft sediment deformation, little sedimentological analysis has ever been attempted, however, commendable work has been carried out by many on postdepositional deformations and metamorphism (e.g. Naha, 1965; Ghosh and Sengupta, 1987; Saha, 1994 and references therein).

3. Facies

The Chaibasa Formation is constituted by three precursor facies, viz.: sandstone (Sst); heterolithic (Hl); and shale (Sh); which are clearly distinguishable on the basis of lithology. The last two finer facies are now transformed into micaschists within which the first facies in the form of conspicuous

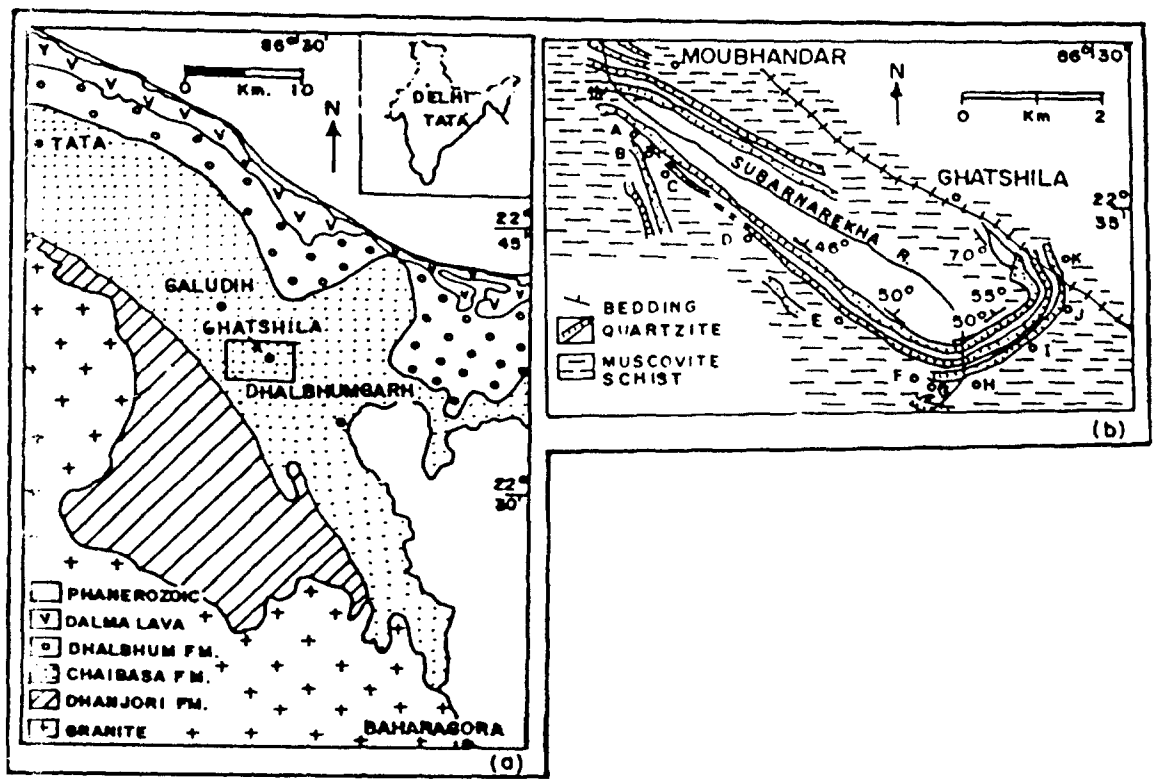

Fig. 1. Outcrop map of the Chaibasa and the bounding formations in eastern India (within inset). Note that the Chaibasa onlaps the granitic basement, overruning the Dhanjori Formation at the south-eastern corner [modified after Saha (1994)]. (a) The rectangle indicates the area where the Sst units were studied. (b) Detailed geology of this area [modified after Naha (1965)]. The solitary letters indicate the locations of the sections illustrated in Fig. 2a.

quartzite ridges are sparsely embedded (Fig. 2a). For the sake of brevity respective descriptions of the facies are presented in Table 2. Only those facies—characteristics which reveal depositional mechanisms and paleogeographies (summarized in Table 2) are discussed below. Emphasis is laid on the Sst facies, wherein the spectacular local preservation of primary features permits the rigorous analysis for the visualization of flow and related bedform dynamics.

3.1. Sandstone facies

The Sst facies units, bounded above and below by micaschists besides being broadly lenticular vary laterally in thickness (Fig. 2a). The rocks are rich in quartz, fine-grained (md = 0.2 mm) and generally well sorted. The facies units generally have their lower and upper contacts sharp with the micaschists. Every facies unit is constituted by numerous intertwined lenticular or wedging Sst bodies separated from each other by marked erosional or non-depositional bounding surfaces. On the basis of their internal structures these constituent Sst bodies can be classified in six subfacies as denoted below.

3.1.1. Subfacies A

3.1.1.1. Description. These fine-grained Sst bodies, characterized by compound cross-stratifications, are wedge shaped. Large (up to 65 cm thick) unidirectional planar cross-sets with down-current decrease in foreset angle from ca 25° to ca 10° give way over a distance of several metres to compound cross-stratification (cf Rouse, 1961;

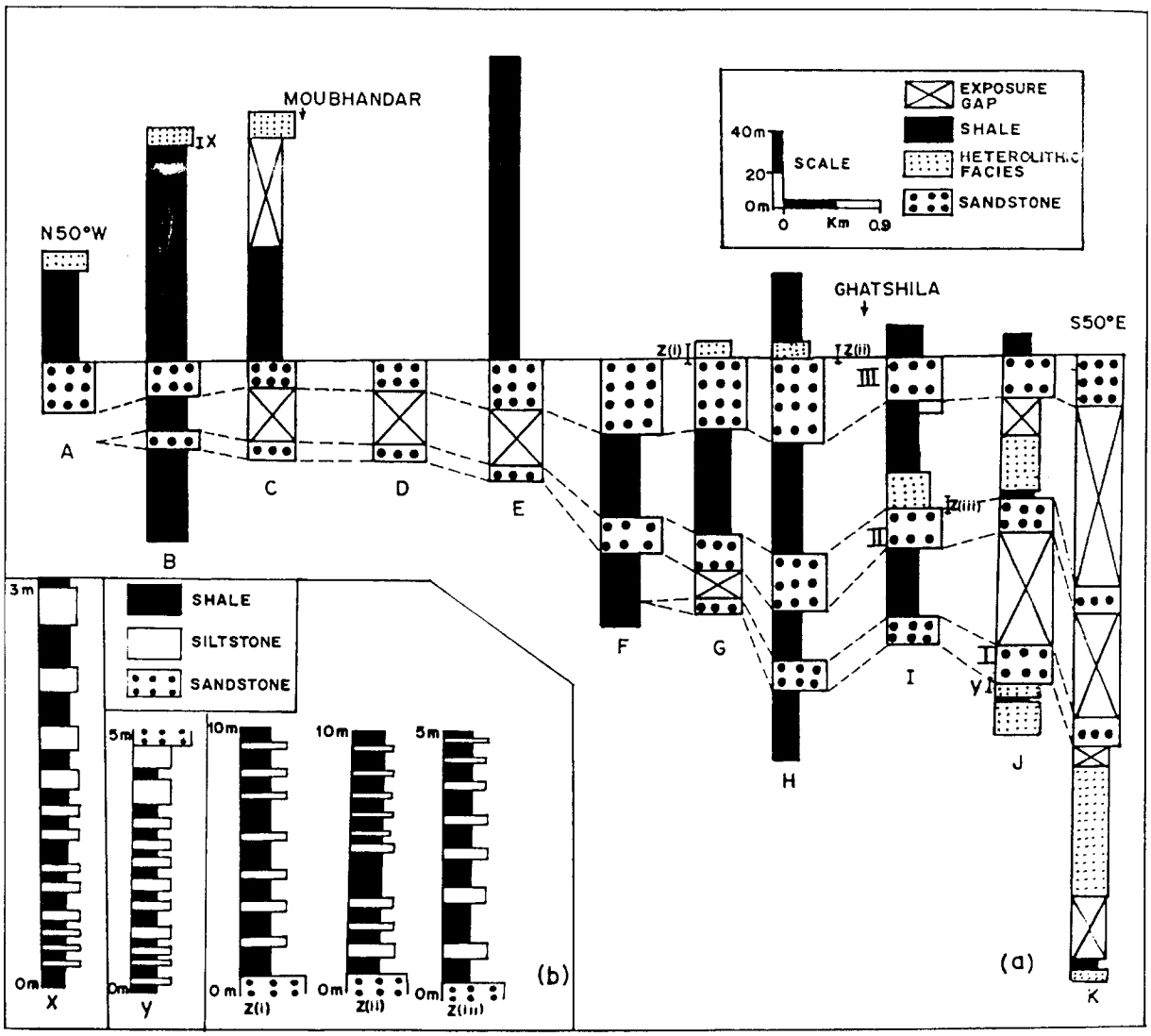

Fig. 2. Facies panel based on sections marked in Fig. 1b. (a) The Sst units, labelled as I, II and III are detailed in Fig. 4. (b) Transitions upward (*z* i,ii,iii) and downward (*y*) from Sst to Hl and upward transition from Sh to Hl (*x*). For locations of these transitions see (a).

Imbrie and Buchenan, 1965) (Fig. 3a). Within the compound cross-stratifications, the smaller cross-lamina sets are ca 3 cm thick and are periodically punctuated by relatively steeper and erosive reactivation surfaces. Between every two reactivation surfaces the cross-lamina style systematically changes downcurrent:

(1) concave-up forms with a strong erosional base, followed by:
(2) tabular forms, partly overstepping the toes of the preceding subset and giving way gradationally to:
(3) progressively gentler sigmoidal forms (Fig. 3b).

Concomitantly the basal surface is elevated and the grain-size diminishes, so much as to often turn the sigmoidal subsets distinctly muddy. Directional reversals between the sets are locally observed.

Table 2
Description of precursor facies

Litho facies	Description	Thickness	Geometry	Vertical contact	Internal structures
Sh	Dark coloured Sh with or without interlayers of siltstone. Channels or scours were present with maximum width and depth 60 and 18 cm, respectively. There was little difference between the sediments within and outside the channels.	Unit thickness ranges >100 m. Sh beds are generally slightly thicker than adjacent siltstones (<4 cm). Overthickened siltstone beds have maximum thickness of 30 cm.	Siltstone interlayers are sheet-like. Overthickened beds have tubular geometry.	Sh–Hl gradational, Sh–Sst invariably sharp. Vertical or lateral transition from a silt-rich to a silt-poor part is graded. Overthickened beds have bases distinctly sharper than the tops.	Siltstone interlayers are massive, graded plane laminated (millimetre-thick) or rippled (a=0.7–1.6 cm; λ=2–6 cm). The ripples are strongly asymmetric in profile and evidently starved. In sh–silt rhythmites, silt in ripples and in plane laminations occur in alternate layers. Simultaneous silt contribution from two separate systems, viz. a suspended and tractive system is indicative in cross-lamina organization. Overthickened beds are massive and balls and pillows are sparsely floated within them; they may have inversely graded traction carpet deposits (on a millimetre scale) at their bases.
Hl	Interbedded sh and siltstone. Overthickened siltstone beds occur intermittently.	Siltstone bed thicknesses range from 5 to 40 cm (commonly 12–15 cm). Sh bed thicknesses are widely variable between 2 and 60 cm.	Thinner siltstone beds are sheet-like; the thicker ones are tabular and lenticular at places.	Hl–Sh contact gradation as the Hl–Sst contacts. The siltstones have sharp bases.	Siltstone beds are cross-stratified or plane laminated (6–15 cm thick), or rippled (a= 0.8–1 cm; λ=5–5.5 cm) often with discernible asymmetry; scour-fill cross-strata (set thickness 6–30 cm) is locally present; hummocky cross-stratifications (a=10–12 cm; λ=1.2–1.5 m) are present at places; scour-fills (width=1–1.5 m; depth=25–30 cm) are massive and/or laminated side-filling. Internal laminations are often secondarily disturbed or obliterated. A locally low angle, slightly concave-up slump scars filled by massive or laminated indigenous sediments, are present. The paleocurrent direction is generally indeterminable owing to deformation.
Sst	Very fine to fine grained locally turned muddy, lenticular, intertwining multiple sandstone bodies of distinctive internal structures constitute a unit.	Unit thickness ranges from 5 to 45 m; and are laterally variable (Fig. 2a). Bed thickness is laterally variable, with the maximum being 2.5 m. The beds are commonly erosion-based.	Units have laterally variable thicknesses with overall lenticular geometry.	Sst–Sh contact is common and invariably sharp. Sst–Hl contacts are rare and gradational, but relatively more common in upward transition.	Thoroughly cross-stratified with the rare incorporation of massive or graded beds and still rarer plane laminations. Tidal rhythms in successive packages defined by mud-linings within the cross-sets. Secondary obliteration of internal structures is a common feature. Locally low angle, slightly concave-up slump scars filled by massive or laminated indigenous sediments, are present.

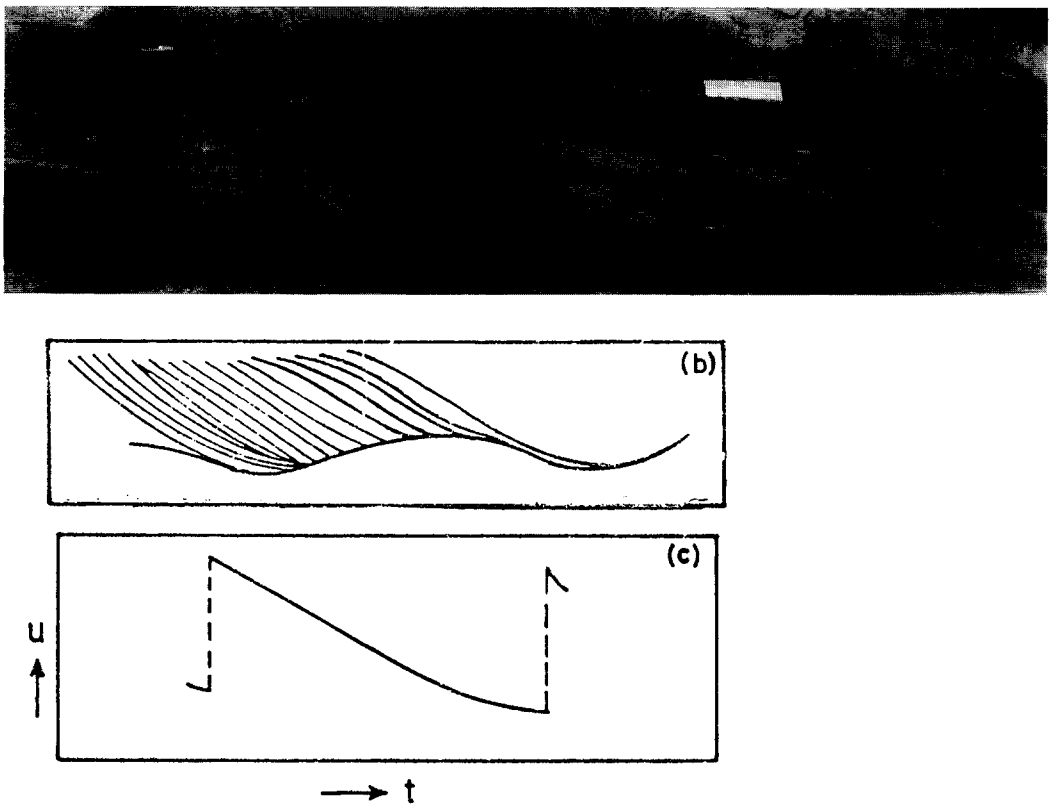

Fig. 3. (a) Cross-stratification in Sst subfacies A gives way downcurrent to compound cross-stratification (arrow) (pencil length 14 cm). (b) Change in cross-stratification style within a cycle of smaller cross-set (idealized, not to scale). Note that a cycle initiates with a basal erosion and concave-up cross-set giving way to a tabular set and then to a sigmoidal set. (c) Corresponding time (t)–velocity (u) pattern.

Subfacies A is best developed at the base of every Sst facies unit.

3.1.1.2. Interpretation. The intraset cyclic cross-laminal changes, along with grain-size, reveal repeated waxing and waning of the water flow (Fig. 3c). This aspect along with paleocurrent reversals favours a tidal interpretation. In contrast the large scale planar foresets are unidirectional implying that flow reversals could leave their imprint only during the abandoning phase of tidal sandwaves [cf Nio (1976) for much larger sandwaves]. Progradation in a tidal setting is thus inferred (cf Nio and Yang, 1991).

3.1.2. Subfacies B

3.1.2.1. Description. This subfacies except being a little more muddy than subfacies A, differs from the latter only by the complete burial of the considerably smaller sandwaves (average height 18 cm) under cross-laminated layers, and progressively tends to be horizontal turning the beds tabular. The beds, which are overall fining upward, are bounded by a mud layer above of maximum thickness up to 2 cm (Fig. 5a). Double mud drapes [Fig. 5b; cf Visser (1980)] are also present within the cross-lamina sets, which cover the sandwaves. Interestingly, all the three studied Sst units are capped by this subfacies (Fig. 4). These cappings also exhibit the stacking of beds of subfacies B. As one progresses up the stacks, the bed-thickness

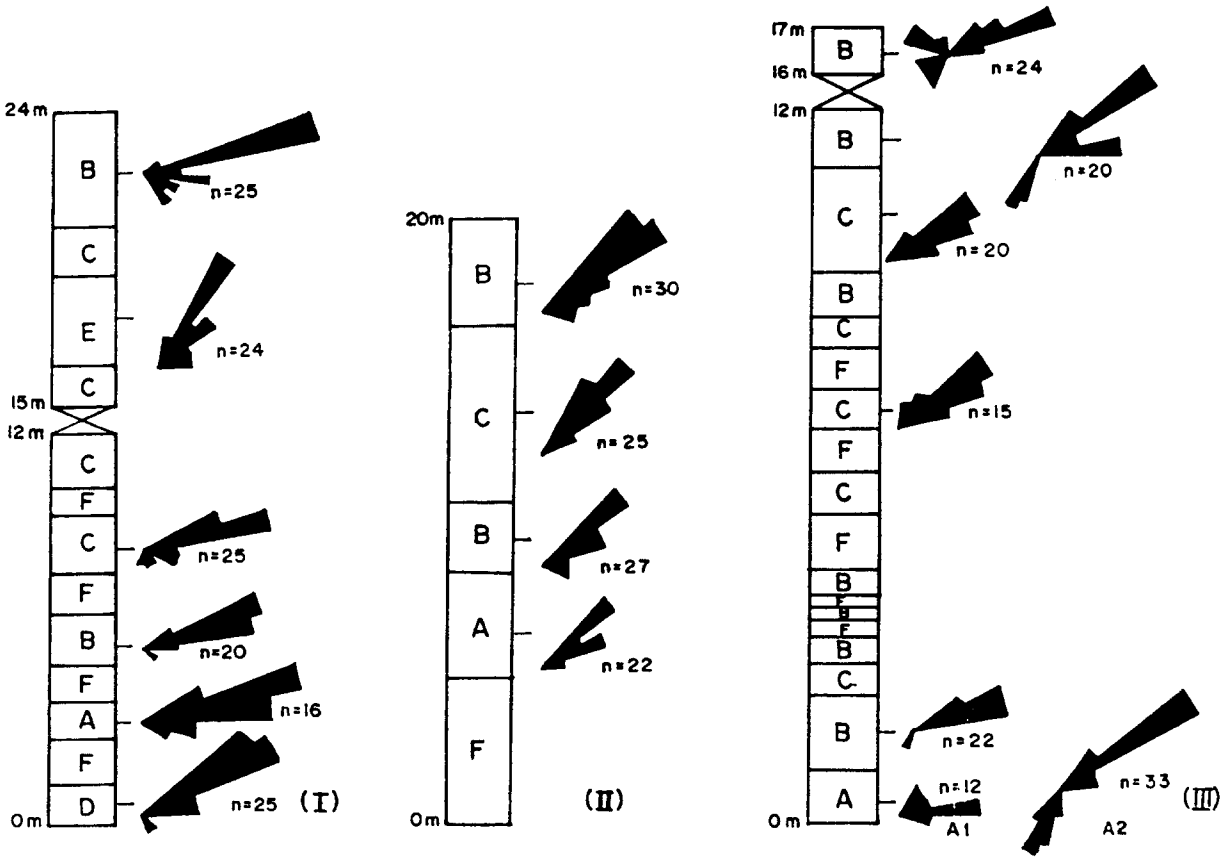

Fig. 4. Subfacies successions within Sst units (locations marked in Fig. 2a and the paleocurrent patterns within them). A_1, larger; and A_2, smaller cross-stratifications in facies A.

decreases with the intervening mud layers becoming more pronounced and the sandwave height being reduced (Fig. 5c). Paleocurrent reversal is locally pronounced.

3.1.2.2. Interpretation. The depositional frame of this subfacies appears to be nearly the same as in subfacies A, but with the overall rapid decline of depositional energy through space as well as time. This results in sandwave abandonment. The double mud drapes are characteristic of tidal influence (Visser, 1980; Mellere and Steel, 1995) and indicate deposition in a subtidal setting (Kohseik and Terwindt, 1981). The architecture of the stacks of subfacies B beds, with ubiquitous double mud drapes at the top of the Sst facies units indicates aggradation or slight retrogradation before giving way upward to a finer facies; commonly Sh (see below).

3.1.3. Subfacies C

3.1.3.1. Description. This subfacies is characterized by sets (average thickness 32 cm) of alternating thick and thin planar tabular cross-stratifications (Fig. 6a). The plotting of successive foreset thicknesses also reveals a larger near-symmetric cyclicity (Fig. 6b). Between the two successive peaks, the number of lamination is, on average, 27. From a peak to the next trough the foreset angle decreases and the paleocurrent pattern is unimodal (Fig. 4).

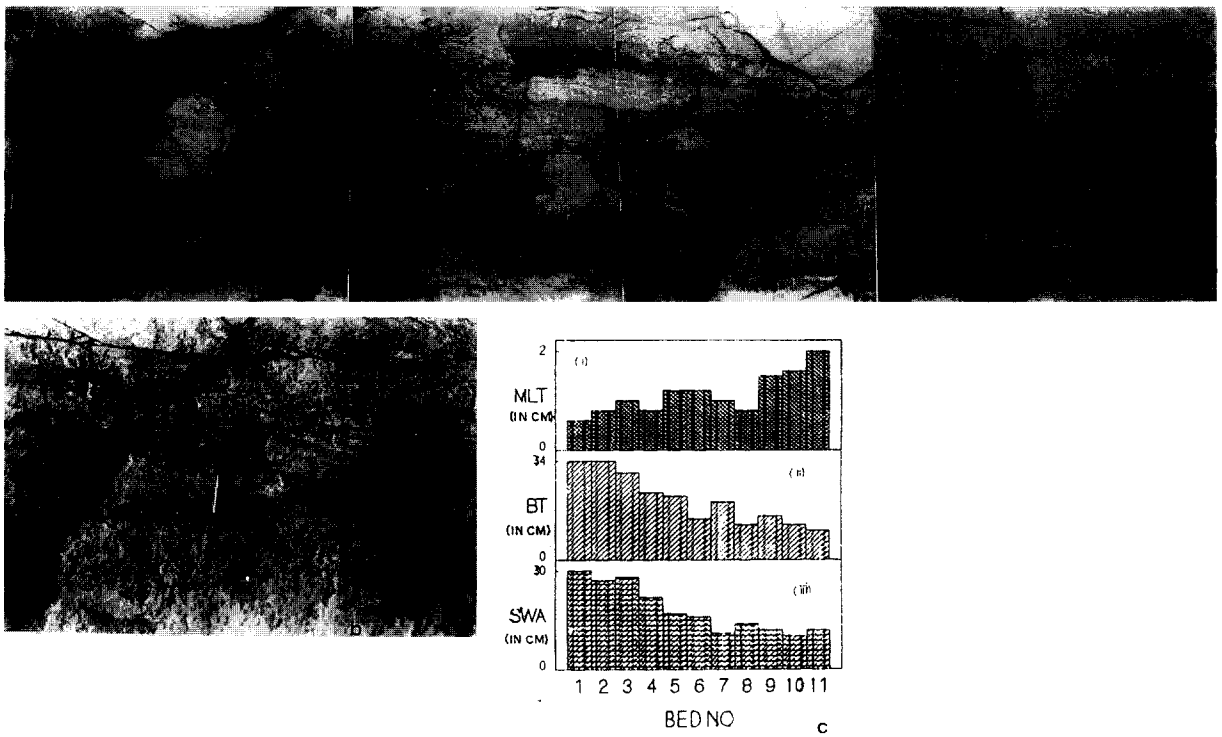

Fig. 5. (a) A small sandwave (inked) and the cross-lamina sets draping over it in Sst subfacies B. The mud drapes bounding the bed are shown by arrows (match stick length 4.2 cm). (b) Double mud drapes within the draping cross-lamina sets (match stick length 4.2 cm). (c) The upward variations within a stack of subfacies B bodies: sandwave height (SWA, nucleus bedform); bed thickness (BT); and bounding mud layer thickness (maximum, MLT).

3.1.3.2. Interpretation. Bedload movement under the influence of a dominant unidirectional current is inferred. The thick–thin foreset alternations superimposed on a larger cycle strongly favour a tidal interpretation (Visser, 1980; De Boer et al., 1989), with the larger cycle being then very compatible with the lunar bi-monthly (spring to spring) cycle. This is strongly corroborated by the periodicities revealed by fast Fourier transformation of another foreset thickness series by Archer et al. (1991) (Fig. 6c).

3.1.4. Subfacies D

3.1.4.1. Description. Cross-stratifications with widely variable set thickness ranging up to 42 cm, constitute roughly tabular bodies. Their style changes in cycles commencing with a basal scour and then immediately followed by a steep (ca 28) foreset with a long top, but no toeset (Fig. 7a and b). A basal brink point arises at the shoulder of the scour. The downcurrent of the topset progressively shortens, and then as a topset appears and progressively lengthens, the brink point moves obliquely upward and the basal surface gradually rises (cf Kreisa and Moiola, 1986). This trend continues until the brink point coincides with the top of the set, resulting in concave-up cross-stratifications. Within the concave-up subset, the toeset continually increases in length as the grain-size decreases, until the trend is reversed both ways. Eventually a sigmoidal cross-strata with continued shortening of the toeset follows, which is compensated by progressive lengthening of the topset. A cycle terminates with appearance of the next basal scour and the complete disappearance of the toeset (Fig. 7b). The number of foresets within a cycle is ca 25–29 and thick–thin alternations are typical

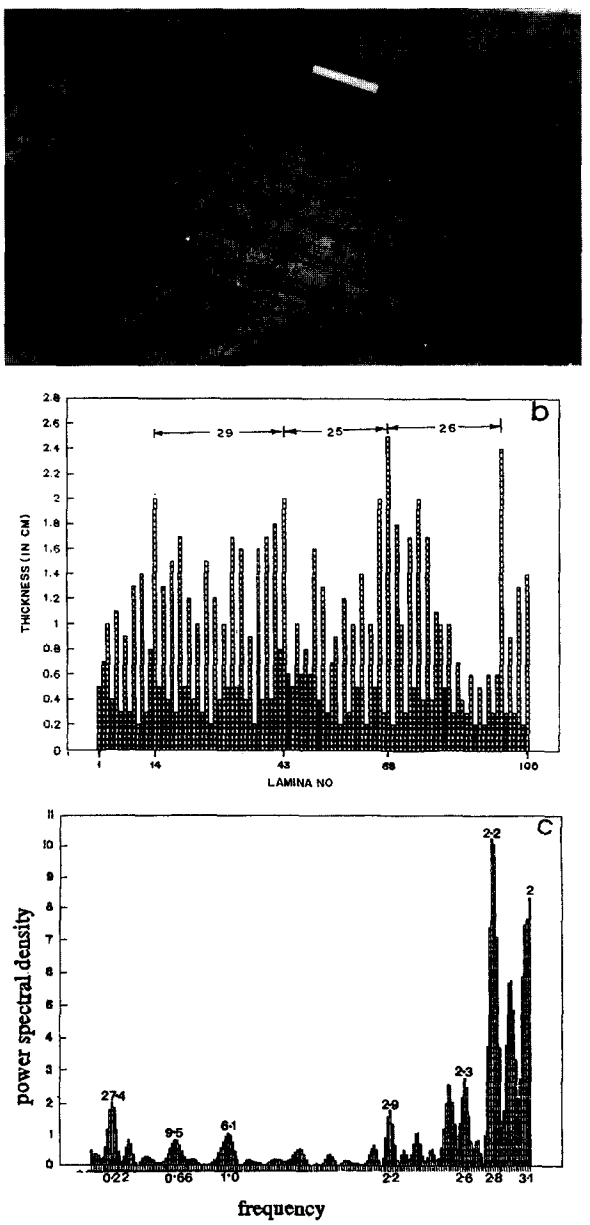

Fig. 6. (a) Thick–thin alternations in large scale cross-stratifications in Sst subfacies C (pen length 12 cm). (b) The plotting of successive foreset thickness depicts a larger cycle. (c) Fast Fourier transformation of a longer forset thickness series: note periodicities at 2 and 27.4.

(Fig. 7d). Double mud drapes are common and the current was unimodal (Fig. 4).

3.1.4.2. Interpretation. The thick–thin alternations as well as the longer cyclic variations in foreset thickness are readily attributable to semidiurnal tides. Fast Fourier transformation of the foreset thickness series further corroborates the tidal periodicities (Fig. 7e). Double mud drapes clearly indicate deposition in a subtidal setting (Visser, 1980). Persistence of either or both, top and toesets indicates sandwave migration under persistent sand fall-out alternately favouring the summit and the trough of the sandwave (cf Chakraborty and Bose, 1992). The intermittent basal scours indicate that the backflow trajectory had hit the toe of the sandwave directly and undercut it, and then gradually moved away only to shift back gradually towards the toe later. Periodic fluctuations in flow velocity (Fig. 7c) and co-ordinated variations in the intensity of backflow and shifting of the suspension fall-out blanket up and down the lee face of the sandwave can thus be envisaged (see Kreisa and Moiola, 1986). Cyclic grain-size variations further corroborate this contention. Nevertheless, the suspension-cloud must have hung well above the bedform to permit flow-detachment at the bedform-crest. The grain-lifting power of a current considerably increases in combination with the waves, hence a wind-generated wave coinciding with the dominant tide seems very likely for generation of this subfacies.

3.1.5. Subfacies E

3.1.5.1. Description. In this roughly tabular fine grained Sst facies the stratification style changes laterally but non-cyclically, as results from accretion on virtually stationary and supercritically climbing sandwaves (maximum height 35 cm; Fig. 8a). The cross-stratifications resulting from lee side accretion are initially spindle-shaped having a brink point immediately beneath the summit [Fig. 8a, cf Swift and Rice (1984); see also Imbrie and Buchenan (1965)]. Unlike the case in subfacies D, the brink point maintains nearly the same vertical distance from the base through lateral accretion, although the depth of base

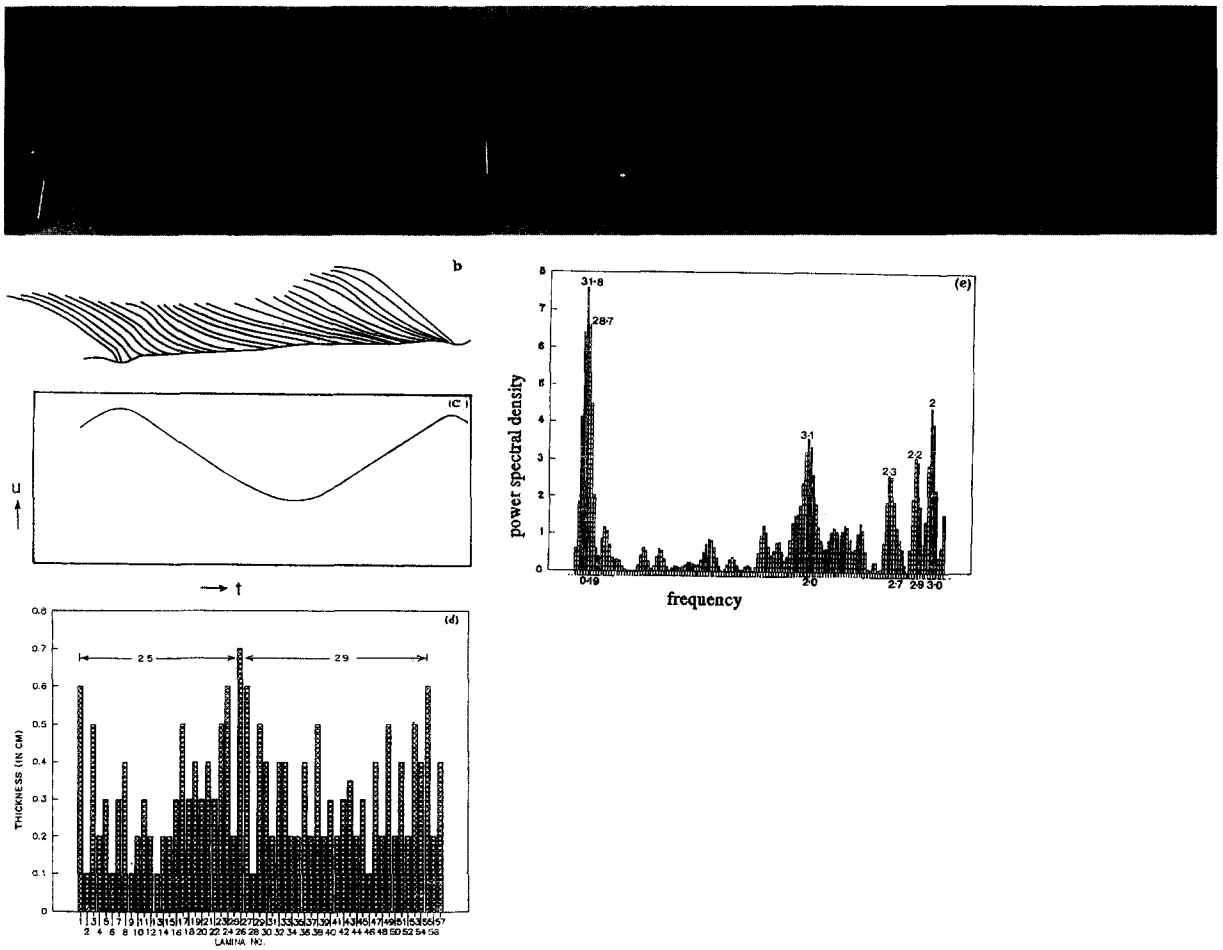

Fig. 7. (a) Cross-set with a brink point gradually rising in the downcurrent direction indicated by match sticks (length 4.2 cm) within Sst subfacies D. (b) The change in cross-stratification style within a cycle in Sst sub facies D (not to scale). (c) Inferred time (t)–velocity (u) pattern within the cycle. (d) Multiple foreset thickness series depicting multiple cycles and (e) its Fast Fourier transformation with notable periodicities at 2 and 31.8.

slightly varies. The horizontal distance between the steeply climbing summit and the brink point thus progressively increases and the consequent suppression of the brink point turns the cross-stratification convex-up, with maximum thickening at the toe. Another downcurrent, the convex-up laminae gradually gives way to millimetre thick quasi-planar stratifications with slight downslope flaring (cf Arnott, 1993). The grain-size decreases only slightly downcurrent over a maximum 3 m exposure length. The lateral variation in lamina-thickness reveals no apparent cyclicity as observed in subfacies B, C or D (Fig. 8c). Within stacks of quasi-planar sets of cross-stratifications bed surfaces locally bear well preserved current crescents (Fig. 8b). Traces of paleocurrent are unimodal (Fig. 4).

3.1.5.2. Interpretation. The rate of sand fall-out from suspension has evidently been much higher than for facies D and steadily increased. In comparison to the facies D situation, the suspension cloud possibly hung close to the sandwave summit, thus inducing tangential flow (without detachment) across the summit (cf Imbrie and Buchenan, 1965; Swift and Rice, 1984) and favouring depos-

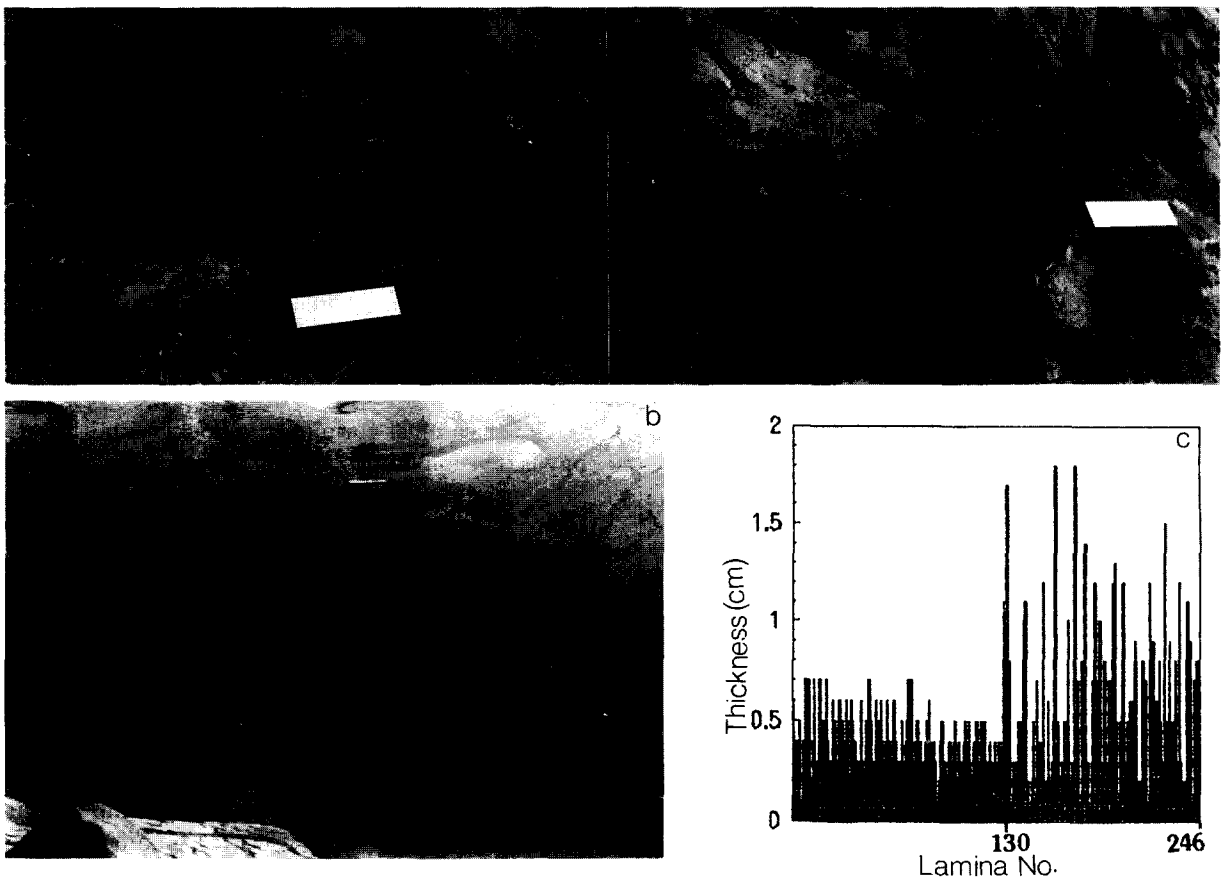

Fig. 8. (a) Lateral transition from spindle to convex-up cross-stratification to quasi-planar stratification in Sst subfacies E. Note brink points (arrows) maintain roughly the same vertical distance from the base which shows slight lateral variation in elevation (scale 16 cm long). (b) Current crescents on bed surface (pen length 16 cm). (c) Lateral foreset lamina-thickness variation does not reflect any cyclic variation.

ition during heavy storms. The unidirectional cross-stratifications point to a tractive current. Nonetheless, rounded crests and distinctly convex-up profiles of the bedforms strongly suggest a combined flow (Harms, 1969; Yokokawa et al., 1995). This suggestion of the wave component seems valid for well preserved hummocky cross-stratifications within the adjacent Hl facies occurring (Table 2, Fig. 9), although their correlation with this subfacies is difficult to establish. Pertinently, Arnott (1993) considered mud-encased quasi-planar sets as products of storm-generated combined flows with a relative dominance of tractive current. The current crescents corroborate the dominance of tractive current of

Fig. 9. Hummocky and swaley cross-stratification in Hl facies (match stick length 4.2 cm).

course, without any paleogeographic connotation (Allen, 1982). The overall characteristics of the subfacies, however, suggest deposition in a subtidal setting.

3.1.6. Subfacies F

3.1.6.1. Description. Rapidly wedging massive or graded Sst of relatively poor sorting gives way upward to current structures in finer fraction (Fig. 10a). Notably, the mineralogical and grain-size spectrum differs little from that of the subfacies assemblage described above. The base of the beds is commonly planar and may have shear folds underneath (Fig. 10b). Immediately above the base, dish structures (cf Lowe and Lopiccolo, 1974) are locally abundant. At places, the base may, however, be deeply incised by gutters of varied dimensions (maximum width and depth 30 and 10 cm, respectively; Fig. 10c). Some gutters are stepped. Isolated diffused packets of cross-stratifications and scour pits are locally observed within the massive part (Fig. 10d). The gutter-fills are commonly massive, but locally crudely cross-stratified. The massive gutter-fills may directly give way upward to plane laminations. The upward transitions from the massive or graded parts to plane and/or ripple laminations are often gradational, lamina persistence being achieved only gradually. The maximum bed thickness recorded was 65 cm.

3.1.6.2. Interpretation. The dish structures point to the rapid settling of grains and the grading indicates a deposition from turbulent suspension. The shear folds underneath attest to strong shear under the flow, indicating something like plug sliding immediately before final rest. The isolated pockets of faint cross-stratifications and scour pits within the massive parts record a high degree of unsteadiness of the flow and the rapid wedging of beds testifies the non-uniform, depletive nature of the flow [Fig. 10e; see Knellar and Branny (1995)]. All these, in cumulation, indicate a hyperconcentrated flow within which the sediment concentration and/or viscosity rapidly changed (Smith and Lowe, 1991). The evidence, particularly that of a very strong shear at the base of the flow, tilts the balance in favour of high-density turbidity currents rather than storm-generated flows. Among the various known mechanisms for triggering submarine massflows earthquake seiches seem to be most probable in close association with abundant soft sediment deformation structures, such as pillows and multilobated convolutes (Fig. 11a), along selected levels, especially within the Hl facies (cf Bose et al., 1997). Deposition under water seems evident.

3.2. Two finer facies

The micaschist forming the background lithology is divisible in two precursor facies, viz. Hl and Sh depending primarily on the thicknesses of the siltstone interbeds within them (see Table 2 and below). The two facies often maintain gradational contacts, laterally and vertically, between themselves.

3.2.1. Heterolithic facies

The siltstone interbeds within the Hl facies commonly vary between 12–15 cm, but may range up to 40 cm. Soft sediment deformation, particularly slumps, are frequently evident within them (Fig. 11b). The beds are, however, commonly parallel-sided and internally cross-stratified, plane laminated, hummocky cross-stratified (Fig. 9) or rippled. The tops of hummocky cross-stratified beds do not bear any evidence of reworking. The ripples are generally distinctly asymmetric. Scours and slump scars are locally present. A few thicker (>15 cm) massive and lenticular siltstone beds with a few floating mud balls occur locally.

3.2.2. Shale facies

Silt intercalations within the Sh facies rarely exceed 4 cm in thickness and are commonly measurable in millimetres. They are either plane laminated and/or rippled. The planar strata, particularly the relatively thicker ones, are distinctly graded (Fig. 12a). The ripples are present in isolated trains, separated by sets of planar laminae. They are distinctly asymmetric and starved. Accretionary laminae on the lee faces of arrested ripples without much climbing is a common feature (Fig. 12b). These accretionary laminae have the

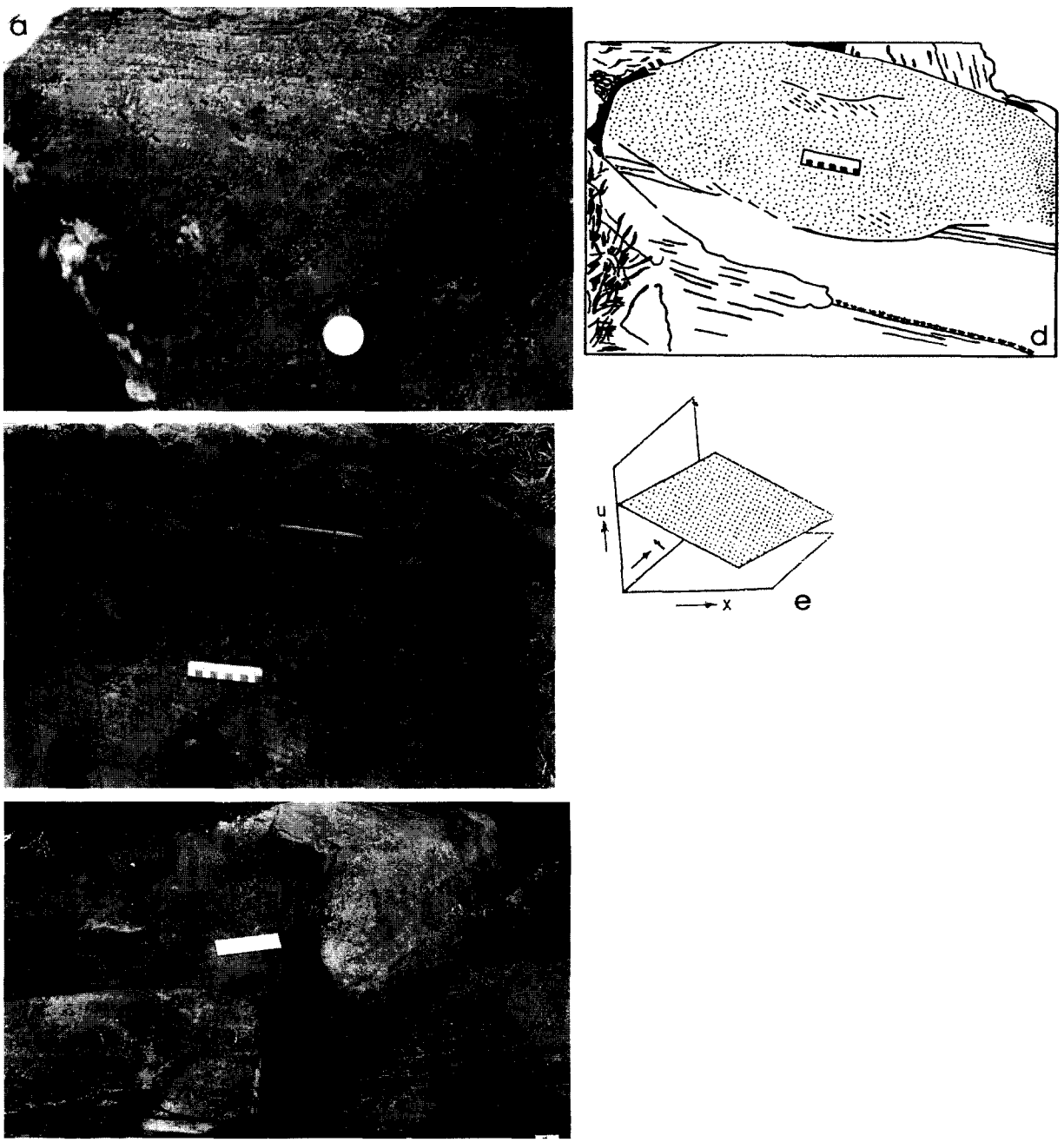

Fig. 10. (a) Graded bed passing over to plane lamination to ripple drift cross-lamination in Sst subfacies F (coin diameter 2.6 cm). (b) Rightward wedging massive bed, delimited by a scale (length 10 cm) and a pen. Note shear folds immediately underneath the scale. Also note that the folding is not accompanied by liquefaction [compare Fig. 165.2D of Mckee et al. (1962)]. (c) A gutter at the base of another massive bed (centre; scale length 16 cm). (d) Erosional base of a massive bed (stippled); note a stepped gutter at bottom and isolated packets of diffused cross-stratifications and scour pits within the bed (sketch from a photograph; scale length 10 cm). (e) Broad change in velocity (u) through space (x) and time (t).

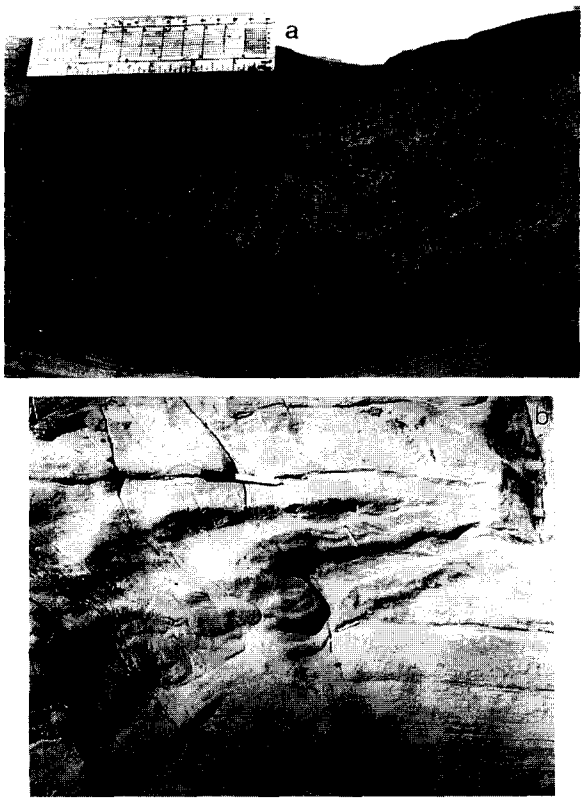

Fig. 11. (a) Multilobated convolute within Hl facies (scale length 16 cm). (b) Slump fold on a steep truncation surface.

same orientation as the ripple lee faces on which they are accreted, but at a progressively lower angle. They tend to fill the ripple troughs passively, not affecting the ripple forms. The ripples and planar laminae of silt alternating with millimetre-thick mud layers give way upward to silt-free Sh with a progressive decrease in the silt content (Fig. 12c). These segments often exceed a metre in thickness and are subdivided in smaller fining upward segments varying in thickness from 6 to 25 cm and those have a ripple train at base, followed up by alternating silt and mud planar laminations. At places, there are small scours (width and depth generally 60 and 18 cm, respectively) and flutes, whose orientations are indeterminable (Fig. 12d). The scours are invariably filled by alternating plane laminations of silt and mud. Local overthickened (< 30 cm) silt beds have their bases sharper than their tops, are internally massive or faintly graded barring millimetre thick inversely graded laminae immediately above the base and balls and pillows sparsely float within them (Fig. 12e). Their bases are planar unless loadcasted.

3.2.3. *Interpretation of the two finer facies*

The complete absence of coarser clastic-filled channels or scours makes a shallow water origin of these finer facies very unlikely. The hummocky cross-stratified siltstone beds are presumably storm products (Harms et al., 1975 and many others). Lack of evidence of fairweather reworking of the storm beds largely confines the paleogeography of the Hl facies between fairweather and storm wave bases.

In contrast, the Sh facies is completely devoid of any wave generated bedform and is likely to be a deeper marine product, formed under the storm wave base. The gradual upward transition of silty segments to silt-free segments of the Sh facies indicates that the silty segments were deposited from episodic overall waning flows, and both silt and mud planar laminae within them are possibly allochthonous. The grading within individual planar silt laminae makes silt deposition from suspension imperative. On the other hand, the single trains of profoundly asymmetric starved ripples imply traction. Accretionary laminae on the ripple lee faces indicate that the traction subsequently became too weak to transport silt as a bedload, yet was still competent to sweep the rain of silt to the lee of the ripples (Fig. 12b). Both traction and suspension seem to have operated closely; yet little climbing of ripples resulted (see Jopling and Walker, 1968). It is imperative that suspension fall-out was permitted only after the cessation of ripple migration, that is, after sufficient weakening of the tractive current. Arguably, two separate transport systems operated: deposition took place from a distal weak current and a stationary suspension cloud [cf Stow and Wetzel (1990) on deep sea hemiturbidites]. In Fig. 12d, a scoured and fluted surface is overlain only by alternations of thin silt and mud. Suspension fall-out of silt is explicit in the silt lamina perfectly mimicking the bottom irregularities, besides local grading. The strong bottom hugging turbulent

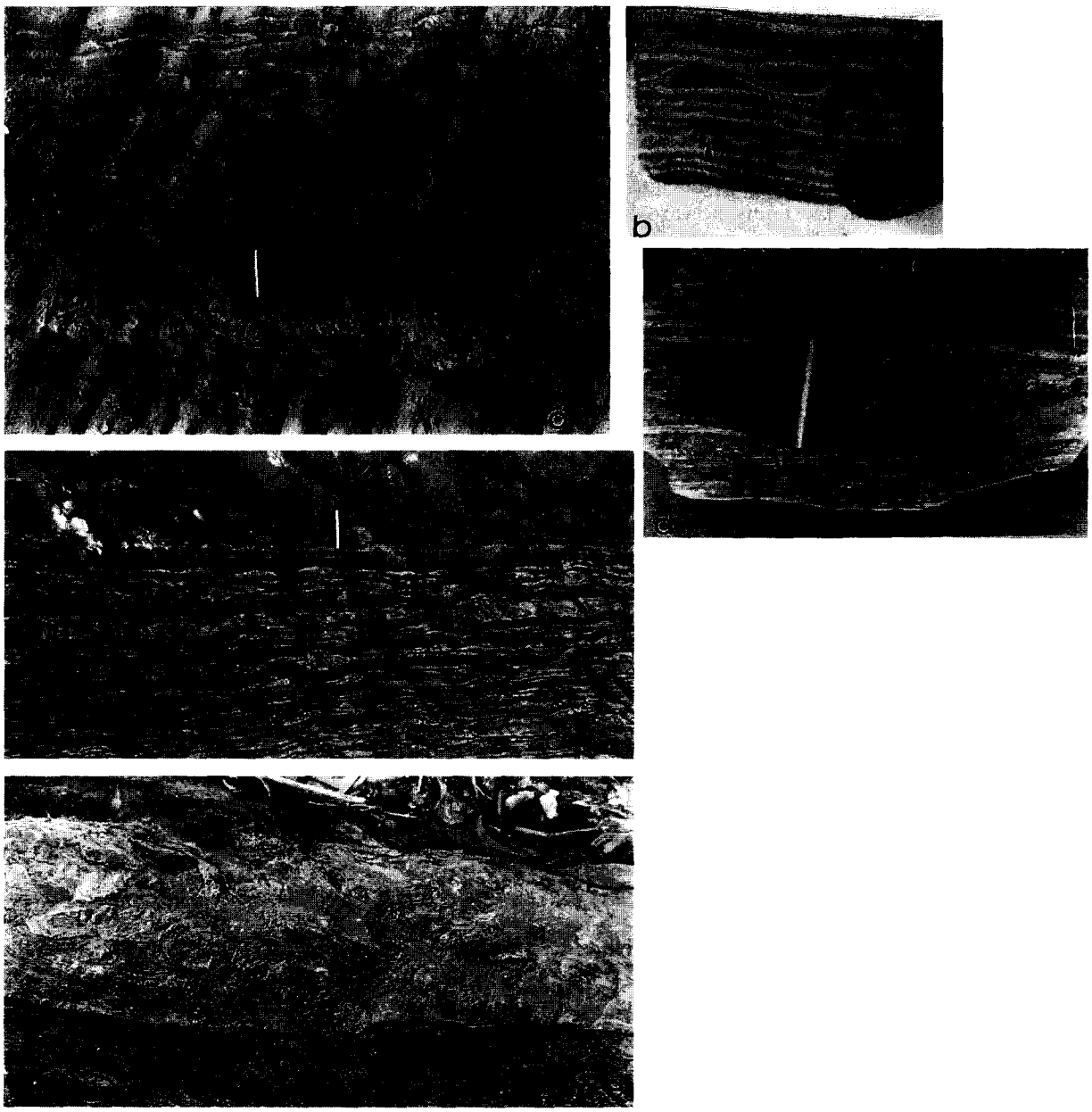

Fig. 12. (a) Grading within two successive siltstone bands within the Sh facies (centre). Note the fossilized ripples at the interface (match stick length 4.2 cm). (b) A smaller silty segment begins (somewhat above the coin, diameter 2.2 cm) with a ripple train, followed up by alternate silt-mud planar laminae. Note the accretionary laminae filling the ripple troughs and the ripple without any tendency to climb and a layer with microloads depicting rapid deposition (arrows). (c) A silty segment grades up into silt-free shale (match stick length 4.2 cm). (d) Scoured surface with flutes (arrows) overlain by silty mud; note the silt lamina draping the bottom irregularities (match stick 4.2 cm long). (e) An overthickened massive bed with detached pillows and thin (light) basal inversely graded traction carpet (immediately above the pen, length 16 cm).

current that caused the erosion and evidently did not deposit anything (bypassed) was conceivably an "efficient" muddy turbidite (Mutti and Ricci Lucchi, 1981).

Repeated switching over from traction to suspension depositional system within the episodic overall waning flow is indicated by the stacks of smaller segments within the fining upward larger silty segments thus envisaging surge-like muddy turbidites. Retrogradational slides or slumps on paleogeographic highs and the liquefaction of the slumped mass to varying degrees may account for the array of transportational-depositional processes visualized (see Mulder and Cochonat, 1996). The overthickened massive or graded beds, irrespective of facies, bear clear attestation to the rapid deposition from the high density massflows. The inversely graded laminae at their bases are presumably traction carpets (Hiscott, 1994).

4. Stratigraphic trend

4.1. Succession

The Chaibasa Formation overlaps the granite basement overrunning the underlying and considerably coarser clastic Dhanjori Formation at the southeastern corner of the given geological map, at the west of Baharagora (Fig. 1a). The Dhanjori Formation is dominated by large-scale cross-stratified, considerably coarser grained, poorly sorted and mineralogically immature terrigenous rocks. On the granitic basement as well as on top of the Dhanjori Formation, the base of the Chaibasa Formation is demarcated by a clast-supported sheet conglomerate with maximum thickness 14 cm (Fig. 13). On the granite basement it is mostly constituted of rounded vein quartz pebbles with maximum length 20 cm. When traced laterally westward into the sediment pile, on top of the Dhanjori Formation its thickness reduces to 3 cm and its composition changes with the incorporation of fragments derived from the substrate and the maximum clast length reduces to 70 mm.

Within the Chaibasa Formation the facies relationships could be worked out in 11 sections

Fig. 13. Sheet-like granular lag of vein quartz and rip-up clast at the contact between the Chaibasa and the underlying Dhanjori. Both the subjacent and superjacent beds are of phylite (chlorite-rich in Dhanjori and muscovite-rich in Chaibasa; match stick length 4.2 cm).

between which only the Sst facies units are, more or less, continuously traceable (Fig. 2b). Lateral intertonguing or gradational transitions between the Sst and the finer facies encasing them was never encountered. In these sections, all but one downward transitions are to Sh, omitting Hl. The only downward transition to Hl is also short (Fig. 2b.*Y*). The upward transitions from the Sst, in the majority of cases, are again to Sh and, where the Hl overlies, it rapidly fines upward [Fig. 2b.*Z*(i), (ii), (iii)]. The vertical transitions between Hl and Sh is generally gradational as exemplified in Fig. 2b.*X*.

The vertical transitions between the different Sst subfacies could be worked out to nearly the full extent within only the three Sst facies units (Fig. 4), although partial observations were made in numerous other sections. The intertwined Sst subfacies give way laterally to each other, but the general observation is that the subfacies A is best developed at the base and subfacies B at the top of the Sst units.

4.2. Paleogeographic shifts

Interpretatively, flow and resultant bedform dynamics varied between subfacies A to E and subfacies F represents massflows within the same Sst units. However, no significant paleogeographic shift is indicated by vertical transitions between

them. Some of them give clear evidence for subtidal deposition and a shallow marine depositional environment can be inferred for Sst in general.

The lateral contacts of Sst with the finer facies is always sharp and without gradation or intertonguing. So the vertical facies transitions are not likely to be results of migration of laterally adjacent facies belonging to, more or less, similar paleobathymetry. A previous discussion on the significant characteristics also indicated deeper bathymetry for the finer facies. The profusion of slump folds and slide scars in conjunction with other structures suggest Hl deposition on a relatively steeper slope, but largely between the fair-weather and storm wave bases. In contrast, Sh bears features indicative of deposition under storm wave base. The vertical facies transitions should thus reflect considerable paleogeographic shifts.

Rapid downward and upward transitions of Sst to the finer facies, commonly to Sh, imply emplacement of the Sst units between the episodes of rapid fall and the rise of relative sea level (RSL), either eustatic or tectonic. The dominance of the progradational subfacies A at the base of the Sst units implies either stillstand or slow rises in RSL at the initial phase of sand deposition. Again, the fining and thinning upward stacks of subfacies B beds at the top of Sst units indicates rising of RSL at a relatively rapid rate during the closing of the sand depositional phases.

The onlapping of the Chaibasa Formation on the granite basement overrunning the Dhanjori Formation with definite shallow water origin is a clear indication of an overall transgressive trend. The thin pebbly or granular sheet at the base of the Chaibasa Formation is thus likely to be of transgressive lag origin. Despite its severe limitation, the available data set identifies an overall transgressive trend, with occasional sharp reversals, as a major deterministic for the Chaibasa sequence building pattern.

5. Conclusion

The Sst facies in the Protoproterozoic Chaibasa Formation, India was emplaced during lowstands in a shallow tide-storm interactive system occasionally disturbed by earthquakes. The flow and related sandwave dynamics varied considerably within the shallow marine paleogeographic frame. Sandy massflows were possibly triggered by earthquakes. Two other finer constituent facies were formed in deeper settings, the relatively coarser one above the storm wave base and the other beneath it. Silty high density flow products and muddy turbidites are common within the finer facies. Repeated lowstands, followed by transgressions, in an overall transgressive frame, apparently controlled the general sequence-building pattern.

Acknowledgements

The authors are greatly indebted to P.L. De Boer and K.A. Eriksson for reviewing an earlier version of the manuscript and suggesting significant improvements. They are also very much indebted to A.W. Archer for providing the methodology for fast Fourier analyses. The financial support came from Project No. ESS/CA/A9-13/92 of the Department of Science and Technology, India to P.K.B. R.M. acknowledges financial support from the University Grants Commission, India. The authors thankfully acknowledge the help they received from Santanu Banerjee and Snehasis Chakrabarty during fieldwork. They acknowledge the infrastructural facilities from their department.

References

Allen, J.R.L., 1982. Sedimentary Structures, Their Character and Physical Basis, Vol. II. Developmental Sedimentology, Chap. 30B. Elsevier, Amsterdam, p. 663.

Archer, A.W., 1996. Reliability of lunar orbital periods extracted from ancient tidal rhythmites. Earth Planet. Sci. Lett. 141, 1–10.

Archer, A.W., Kvale, E.P., Johnson, H.R., Analysis of modern equatorial tidal periodicities as a test of information encoded in ancient tidal rhythmites. In: Smith, D.G., Reinson, G.E., Zaitlin, B.A., Rahmani, R.A. (Eds.), Clastic Tidal Sedimentology (special issue). 1991. Can. Soc. Pet. Geol. Mem. 16, 189–196.

Arnott, R.C., 1993. Quasi-planar laminated sandstone beds of the lower Cretaceous Bootlegger Member, North Central

Montana: evidence of combined flow sedimentation. J. Sedim. Petrol. 63, 488–494.

Basu, A., 1985. Structure and stratigraphy in and around S.E.-part of Dhanjori Basin, Singhbhum, Bihar. Rec. Geol. Surv. India 113, 59–67.

Bhattacharya, H.N., 1991. A reappraisal of the depositional environment of the Precambrian metasediments around Ghatshila-Galudih, Eastern Singhbhum. J. Geol. Soc. India 37, 47–54.

Bose, M.K., 1994. Sedimentation pattern and tectonic evolution of the Proterozoic Singhbhum Basin in the eastern Indian shield. Tectonophysics 231, 325–346.

Bose, P.K., Banerjee, S. and Sarkar, S., 1997. Slope-controlled seismic deformation and tectonic framework of deposition: Koldaha Shale, India. Tectonophysics 269, 151–169.

Chakraborty, C., Bose, P.K., 1992. Ripple/dune to upper stage plane bed transition: some observation from the ancient record. Geol. J. 27, 249–259.

Chan, M.A., Kvale, E.P., Archer, A.W., Sonett, C.P., 1994. Oldest direct evidence of lunar-solar tidal forcing encoded in sedimentary rythmites. Proterozoic Big Cottonwood Formation, central Utah. Geology 22, 791–794.

De Boer, P.L., Oost, A.P., Visser, M.J., 1989. The diurnal inequality of the tide as a parameter for recognising tidal influences. J. sedim. Petrol. 59, 912–921.

Gaal, G., 1964. Precambrian Flysch and Molasse-Tectonics and sedimentation around Rakha Mines and Jaikan in Singhbhum District, Bihar, India. Proc. 22th Int. Geol. Cong. 22, 331–356.

Ghosh, S.K., Lahiri, S., 1983. Morphology and penecontemporaneous interpenetrative contortions and their modification by diastrophic movements in the Ghatshila-Galudih area. Singhbhum, Eastern India. In: Rec. Res. Geol., Vol. 10 (Structure and Tectonics of the Precambrian rocks). Hindustan, Delhi, pp. 144–157.

Ghosh, S.K., Sengupta, S., 1987. Progressive development of structures in a ductile shear zone. J. Struct. Geol. 9, 277–287.

Gupta, A., Basu, A., Singh, S.K., 1985. Stratigraphy and petrochemistry of Dhanjori Greenstone belt, Eastern India. Q. J. Geol. Min. Met. Soc. India 57, 248–263.

Harms, J.C., 1969. Hydraulic significance of some sand ripples. Geol. Soc. Am. Bull. 80, 363–396.

Harms, J.C., Southard, J.B., Spearing, D.R., Walker, R.G., 1975. Depositional environments as interpreted from primary sedimentary structures and stratification sequences. S.E.P.M. short course No. 2., p. 161.

Hiscott, R.N., 1994. Traction-carpet stratification in turbidites—fact or friction? J. Sedim. Res. A64, 204–208.

Imbrie, J., Buchenan, H., 1965. Sedimentary structures in modern carbonate sands of the Bahamas., In: G.W. Middleton (Editor), Primary Sedimentary Structures and their hydrodynamic Interpretation.. Soc. Econ. Paleo. Min. Spec. Publ. 12, 149–172.

Jopling, A.V., Walker, R.G., 1968. Morphology and origin of ripple-drift cross-lamination with examples from the Pleistocene Massachusetts. J. Sedim. Petrol. 38, 971–984.

Knellar, B.C., Branny, M.J., 1995. Sustained high-density turbidity currents and the deposition of thick massive sands. Sedimentology 42, 607–616.

Kohseik, L.H.M., Terwindt, J.H.J., 1981. Characteristics of foresets and topset bedding in megaripples related to hydrodynamic conditions on an intertidal shoal. Int. Assoc. Sediment. Sp. Publ. 5, 27–37.

Kreisa, R.D., Moiola, R.J., 1986. Sigmoidal tidal bundles and other tide-generated sedimentary structures of the Curtis Formation, Utah. Geol. Soc Am. Bull. 97, 381–387.

Lowe, D.R., Lopiccolo, L.D., 1974. The characteristics and origins of Dish and Pillar Structure. J. Sedim. Petrol. 44, 484–501.

Mathur, S.M., 1960. Turbidites and sedimentary structures from Chaibasa Stage, Iron Ore Series. Proc. 47th Indian Sci. Cong. Pt III (Abs.), p. 267.

Mckee, E.D., Reynolds, M.A., Baker, C.H., 1962. Experiments on intraformational recumbent folds in cross-bedded sand. U.S. Geol. Surv. Prof. Paper 450-D, D155–D160.

Mellere, D., Steel, R.J., 1995. Facies architecture and sequentiality of nearshore and shelf sandbodies: Haystack Mountain Formation, Wyoming, U.S.A.. Sedimentology 42, 551–574.

Mulder, T., Cochonat, P., 1996. Classification of offshore mass movement. J. Sedim. Res. 66, 43–57.

Mutti, E., Ricci Lucchi, F., 1981. Introduction to the excursions on siliclastic turbidites. 2nd International Association of Sedimentologists European Regional Meeting Excursion Guidebook, Bologna. Blackwell Scientific Publications, Oxford, pp. 1–3.

Naha, K., 1956. Penecontemporaneous Deformation in the Pre-Cambrian Metasedimentary Rocks in Dhalbhum, Bihar. Q. J. Geol. Min. Metal. Soc. India. XXVIII, 155–157.

Naha, K., 1961. Precambrian sedimentation around Ghatshila in East Singhbhum, Eastern India. Proc. Nat. Inst. Sci. India. 27, 361–372.

Naha, K., 1965. Metamorphism in relation to stratigraphy, structure and movements in parts of east Singhbhum, Eastern India. Q. J. Geol. Min. Metal. Soc. India 37, 41–88.

Nio, S.D., 1976. Marine transgression as a factor in the formation of sandwave complexes. Geol. Mijnb. 55, 18–40.

Nio, S.D., Yang, C.S., 1991. Sea-level fluctuations and the geometric variability of the tide dominated sandbodies. Sedim. Geol. 70, 161–193.

Rouse, R., 1961. Fluid Mechanics For Hydraulic Engineers. Dover, New York.

Saha, A.K., 1994. Crustal evolution of Singhbhum–North Orissa, Eastern India. Geol. Soc. India Mem. 27, 341

Saha, A.K., Ray, S.L., Sarkar, S.N., 1988. Early history of the Earth: evidence from the Eastern Indian Shield. In: Mukhopadhyay, D. (Ed.) Precambrian of the Eastern Indian Shield (special issue). Geol. Soc. India Mem. 8, 13–37.

Sarkar, S.C., 1984. Geology and Ore mineralisation of the Singhbhum Copper–uranium belt, Eastern India, Jadavpur University, Calcutta, p. 263.

Sarkar, S.C., Gupta, A., Basu, A., 1992. North Singhbhum Proterozoic Mobile Belt, Eastern India: its Character, Evolution and Metallogeny. In: Sarkar, S.C. (Ed.)

Metallogeny Related to Tectonics of the Proterozoic Mobile Belts. Oxford and IBH, New Delhi, pp. 271–305.

Sarkar, S.N., Saha, A.K., 1962. A revision of the Precambrian stratigraphy and tectonics of Singhbhum and adjacent region. Q. J. Geol. Min. Metal. Soc. India 34, 97–136.

Sarkar, S.N., Saha, A.K., 1986. Stratigraphy, tectonics and geochronology of the Singhbhum region and copper belt shear zone. In: Sarkar, S.N. *et al.* (Eds.). Geology and Geochemistry of Sulphide Orebodies and Associated Rocks in Mosaboni and Rakha Mines Sections in the Singhbhum Copper Belt. Indian School of Mines, Dhanbad, pp. 5–17.

Smith, G.A., Lowe, D.R., 1991. Lahars: volcano-hydrologic events and deposition in the debris flow–hyperconcentrated flow continuum. In: Fisher, R.V., Smith, G.A. (Eds.), Sedimentation in Volcanic Settings. Soc. Econ. Paleo. Min. Sp. Publ. 45, 59–70.

Sonett, C.P., Kvale, E.P., Zakharian, A., Chan, M.A., Demko, T.M., 1996. Late Proterozoic and Paleozoic tides, retreat of the Moon, and Rotation of the Earth. Science 273, 100–104.

Stow, D.A.V., Wetzel, A., 1990. Hemiturbidite: a new type of deep water sediment. Proc. DSDP 116, 25–34.

Swift, D.J.P., Rice, D.D., 1984. Sand bodies on muddy shelves: a model for sedimentation in the western interrior Cretaceous Seaway, North America. In: Tillman, R.W., Siemers, C.T. (Eds.), Siliclastic Shelf Sediments. Soc. Econ. Paleo. Min. Spec. Publ. 34, 43–62.

Virnave, S.N., Mukhopadhaya, T.K., Krishnabadri, N.S.R., 1994. On some aspects of stratigraphy, depositional environment and its bearing on uranium mineralisation in parts of Singhbhum Shear Zone, Bihar. J. Geol. Soc. India 43, 557–571.

Visser, M.J., 1980. Neap-spring cycles reflected in holocene subtidal large-scale bedform deposits: a preliminary note. Geology 8, 543–546.

Williams, G.E., 1989. Tidal rhythmites: geochronometer for the ancient Earth–Moon system. Episodes 12, 162–171.

Yokokawa, M., Masuda, F., Endo, N., 1995. Sand particle movement on migrating combined-flow ripples. J. Sedim. Res. A65, 40–44.